Efficient yellow Dy:ZBLAN fiber laser with highbrightness diode-pumping at 450 nm

Jonathan Demaimay, Esrom Kifle, Pavel Loiko, Florence Pau, Gilles Recoque, Thierry Georges, Thiphaine Rault, Laurine Bodin, Franck Joulain, Patrice Camy, et al.

▶ **To cite this version:**

Jonathan Demaimay, Esrom Kifle, Pavel Loiko, Florence Pau, Gilles Recoque, et al.. Efficient yellow Dy:ZBLAN fiber laser with highbrightness diode-pumping at 450 nm. Optics Letters, 2024, 49 (15), pp.4174. 10.1364/OL.529025 . hal-04776018

HAL Id: hal-04776018
https://hal.science/hal-04776018v1

Submitted on 10 Nov 2024

HAL is a multi-disciplinary open access archive for the deposit and dissemination of scientific research documents, whether they are published or not. The documents may come from teaching and research institutions in France or abroad, or from public or private research centers.

L'archive ouverte pluridisciplinaire **HAL**, est destinée au dépôt et à la diffusion de documents scientifiques de niveau recherche, publiés ou non, émanant des établissements d'enseignement et de recherche français ou étrangers, des laboratoires publics ou privés.

Efficient yellow Dy:ZBLAN fiber laser with high-brightness diode-pumping at 450 nm

JONATHAN DEMAIMAY,[1] ESROM KIFLE,[1,2] PAVEL LOIKO,[1] FLORENCE PAU,[2] GILLES RECOQUE,[2] THIERRY GEORGES,[2] THIPHAINE RAULT,[3] LAURINE BODIN,[3] FRANCK JOULAIN,[3] PATRICE CAMY,[1] AND ALAIN BRAUD[1,*]

[1]*Centre de Recherche sur les Ions, les Matériaux et la Photonique (CIMAP), UMR 6252 CEA-CNRS-ENSICAEN, Université de Caen Normandie, 6 Boulevard Maréchal Juin, 14050 Caen, France*
[2]*Oxxius SA, 4 rue Louis de Broglie 22300 Lannion, France*
[3]*Le Verre Fluoré, rue Gabriel Voisin, Campus de Ker-Lann, 35170 Bruz, France*
*alain.braud@ensicaen.fr

Received XX Month XXXX; revised XX Month, XXXX; accepted XX Month XXXX; posted XX Month XXXX (Doc. ID XXXXX); published XX Month XXXX

We report on a low-threshold efficient yellow Dy fiber laser with good beam quality featuring high-brightness pumping. It employs a single-clad 0.2 mol% Dy:ZBLAN fiber pumped by two 450-nm blue GaN laser diodes. The continuous-wave Dy-fiber laser delivers a maximum output power of 109 mW at 575 nm with a laser threshold of 218 mW, a slope efficiency of 19.6%, and beam quality factors $M^2_{x,y}$ ~1.5. The overall optical efficiency versus incident pump power is 13.9%, being record-high for this type of lasers. The laser performance is simulated based on the spectroscopic data, being in good agreement with the experiment. © 2024 Optical Society of America

http://dx.doi.org/10.1364/OL.99.099999

Nowadays, there is a great demand for coherent light sources emitting in the yellow, at wavelengths ranging from 565 to 590 nm, due to their applications in medicine, astronomy, novel imaging methods and display technologies. In ophthalmology, 577 nm lasers enable gentle treatment because of weak light scattering and strong absorption of melanin and oxyhemoglobin allowing the use of low-power radiation [1]. Additionally, narrow-linewidth yellow lasers emitting at 589 nm find utility in laser guide stars to correct wavefront perturbation of light as it passes through the atmosphere using the D_2 line of sodium ions [2].

Currently, there exist different ways to generate yellow light, *e.g.*, by using dye lasers, copper vapor lasers, of systems employing nonlinear frequency conversion often coupled with Raman effect [3,4]. Pask and Pieper reported on an intracavity frequency doubled Nd:YAG / $LiIO_3$ Raman laser delivering 1.2 W at 578 nm [3]. Despite offering substantial output powers, these laser schemes impose complex and expensive design and maintenance.

Direct generation of yellow emission from a solid-state laser can be attained using trivalent dysprosium ions (Dy^{3+}) [5,6]. Dy^{3+} (electronic configuration: $[Xe]4f^9$) exhibits a metastable state $^4F_{9/2}$ separated by a large energy gap (~7400 cm^{-1}) from a ground of lower-lying multiplets ^6H_J and ^6F_J. The transitions to these levels give rise to multicolor visible emissions, out of which the $^4F_{9/2} \rightarrow {}^6H_{13/2}$ one corresponding to the maximum luminescence branching ratio (and, consequently, highest the emission intensity) [7] falls in the yellow spectral range, see Fig. 1(a). The development of yellow Dy lasers faces a number of problems arising from the spectroscopic behavior of Dy^{3+} ions. First, they suffer from self-quenching via several cross-relaxation (CR) processes that prevent the use of high doping concentrations in laser gain materials [8]. Second, although Dy^{3+} ions absorb blue light at 450 nm (in the spectral range addressed by commercial GaN-based diodes), their absorption cross-sections are very low because of the spin-forbidden nature of the corresponding transition, $^6H_{15/2} \rightarrow {}^4I_{15/2}$ [9]. Finally, especially for low-phonon energy materials, the lifetime of the terminal laser level $^6H_{13/2}$ is non-negligible [7] resulting in resonant excited state absorption (ESA) at the laser wavelength often causing a self-pulsing laser behavior [5].

There exist studies on bulk yellow Dy lasers, mainly employing Dy:$LiLuF_4$ and Dy:YAG [9,10]. The relatively high position of the excited configuration $4f^85d^1$ of Dy^{3+} prevents interconfigurational ESA and enables the use of oxide matrices. Bowman *et al.* reported on a Dy:YAG laser pumped by a 447-nm GaN diode generating 150 mW at 583 nm with a relatively low slope efficiency of 12% [9]. The development of bulk yellow Dy-lasers is mainly limited by the low pump absorption efficiency and the need for cm-long crystals.

Thus, the fiber laser design appears as a natural solution for enhancing the pump absorption. Fiber lasers also offer the advantages of good beam quality and distributed thermal management. Specifically, rare-earth-doped fluoride fibers (e.g., based on ZBLAN glasses) are appealing for visible lasers owing to

their broadband transparency, low refractive index, low phonon energy behavior, and intrinsically long luminescence lifetimes.

Yellow Dy:ZBLAN fiber lasers are known [11-15]. Limpert *et al.* first reported on the continuous-wave (CW) operation of this type of lasers by using a 457-nm Ar^+-ion laser as a pump source: the Dy-fiber laser yielded 10 mW at 575 nm with a slope efficiency of 1.5% [11]. Further improvement of the laser performance was achieved by Wang *et al.* by employing blue GaN diode pumping at 447 nm: the authors extracted 142 mW at 575 nm and with a laser threshold of 250 mW and an optical efficiency of 7.1% [13]. The recent work of Zou *et al.* demonstrated a proof-of-concept of Watt-level yellow lasers using GaN diode-pumped Dy^{3+}-doped ZBLAN fibers [14]. However, owing to the low-brightness pumping, the Dy-fiber laser showed poor beam quality ($M^2 \approx 6$), high threshold (~2.1 W from the laser diode) and an optical efficiency of 9.4%. Takahashi *et al.* proposed a Dy-fiber laser design featuring a very low threshold of 16 mW but with a low output power of 24 mW [15]. These results demonstrate there is still an existing challenge of improving the overall (optical-to-optical) laser efficiency and output beam quality of fiber lasers based on Dy^{3+}-doped ZBLAN fibers.

In the present work, we report on an efficient yellow Dy:ZBLAN fiber laser with high output beam quality featuring high-brightness pumping by single-mode blue laser diodes emitting at 450 nm.

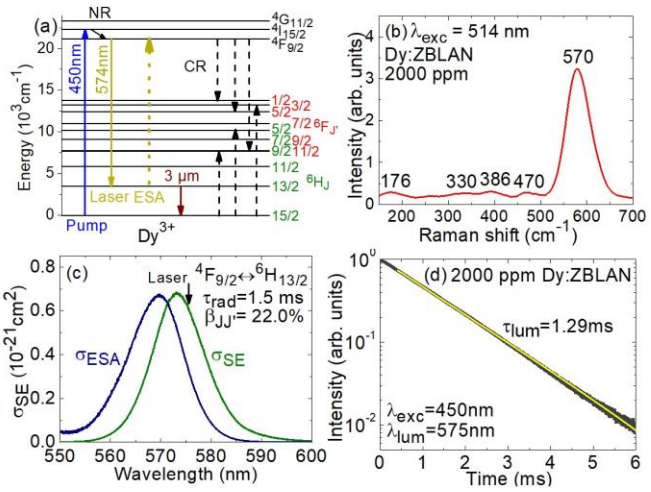

Fig. 1. Spectroscopy of Dy^{3+} ions in the ZBLAN glass: (a) energy-level scheme of Dy^{3+} showing pump and laser transitions, NR – non-radiative relaxation, ESA – excited-state absorption, CR – cross-relaxation; (b) μ-Raman spectrum of the core area of the 2000 ppm Dy:ZBLAN fiber; λ_{exc} = 514 nm, *numbers* - phonon energies in cm^{-1}; (c) stimulated-emission (SE), σ_{SE}, and ESA, σ_{ESA}, cross-sections for the $^4F_{9/2} \leftrightarrow {}^6H_{13/2}$ transition; (d) luminescence decay curve from the $^4F_{9/2}$ state in the 2000 ppm Dy^{3+}-doped fiber, λ_{exc} = 450 nm, λ_{lum} = 575 nm.

First, the spectroscopic properties of the Dy^{3+}-doped ZBLAN glass fiber were characterized. The μ-Raman spectrum measured from the fiber core is shown in Fig.1(b). The dominant Raman band at ~570 cm^{-1} belongs to the Zr – F symmetric stretching vibrations [16]. The stimulated-emission (SE) cross-sections, σ_{SE}, for the $^4F_{9/2} \rightarrow {}^6H_{13/2}$ laser transition in the yellow spectral range were calculated via the Füchtbauer-Ladenburg equation using the radiative lifetime of the $^4F_{9/2}$ state (τ_{rad} = 1.5 ms) and the luminescence branching ratio ($\beta_{JJ'}$ = 22%) previously obtained by the Judd-Ofelt theory [7], Fig. 1(c). The maximum σ_{SE} of 0.69×10^{-21} cm^2 is found at 573 nm, corresponding to an emission bandwidth (FWHM) of 12 nm. Due to a non-negligible lifetime of the terminal laser level $^6H_{13/2}$ (~650 μs [7]), the resonant excited-state absorption (ESA) must be considered. The ESA cross-sections, σ_{ESA}, were calculated by the reciprocity method, assuming a zero-phonon-line (ZPL) energy E_{ZPL} of 17500 cm^{-1} [17] giving an estimate for the reabsorption cross-section at the laser wavelength, $\sigma_{ESA} = 0.37\times10^{-21}$ cm^2 at 575 nm. The luminescence decay curve from the $^4F_{9/2}$ manifold was measured for a 2000 ppm Dy:ZBLAN fiber under pulsed pumping by a blue 450-nm GaN diode, as shown in Fig. 1(d). The decay is nearly single-exponential indicating a weak effect of cross-relaxation for the selected Dy doping level. The luminescence lifetime τ_{lum} is 1.29 ms, indicating a high quantum efficiency ($\eta_q = \tau_{lum}/\tau_{rad}$ = 86%) in line with the low phonon energy behavior of the ZBLAN host matrix.

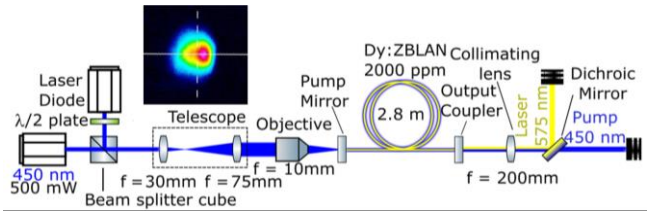

Fig. 2. Layout of the diode-pumped yellow Dy:ZBLAN fiber laser, *inset* – profile of the pump beam.

The laser set-up is depicted in Fig. 2(a). A Dy:ZBLAN single-clad fiber (core / cladding diameters: 16 / 250 μm) from *Le Verre Fluoré* was used as an active medium. The fiber core was doped with 2000 ppm Dy^{3+}, and its length was in the range of 0.9 - 2.8 m. The numerical aperture (N.A.) of the fiber was 0.18. The fiber was strongly multimode at both the pump and laser wavelengths. The fiber end-facets were right-angle cleaved and left uncoated. A linear laser cavity was formed by two external plane mirrors, namely a dichroic pump mirror (PM) coated for high transmission (HT) at the pump wavelength (T > 99% at 450 nm) and high reflection (HR) at the laser one (HR, R >99% at 575 nm), and a set of output couplers (OCs) having a transmission T_{OC} at 575 nm in the range of 5.6% to 67%. Both cavity mirrors were aligned orthogonal to the fiber and placed next to its end-facets. For pumping, two identical single-emitter GaN blue laser diodes (*Oxxius*) were used. Each of them emitted up to 500 mW at 449.5 nm with linearly polarized radiation and a near diffraction limited beam (measured M^2 = 1.14). Their output was combined using an antireflection (AR) coated half-wave plate and a beamsplitter cube. The pump beam was first expanded using a telescope comprising two AR-coated achromatic lenses (f = 30 mm and 75 mm) and then coupled into the fiber through the PM using a microscope objective (f = 10 mm). The measured pump spot size was 5.7(x)×4.6(y) μm^2 at the entrance of the fiber (core pumping). Considering certain losses of the pump radiation in the coupling optics, the maximum incident pump power amounted to 785 mW. Then ,the yellow laser emission was collimated using an AR coated lens (f = 200 mm) and separated from the residual pump using a 45° oriented highly reflective dichroic mirror. The pump absorption efficiency under lasing condition $\eta_{abs,L}$ was determined by measuring the residual pump power after the dichroic mirror. At the maximum P_{inc}, $\eta_{abs,L}$ decreased for shorter fiber lengths, from 99.5% (L = 2.8 m) to 89.6% (L = 0.9 m). Very weak ground-state bleaching was observed.

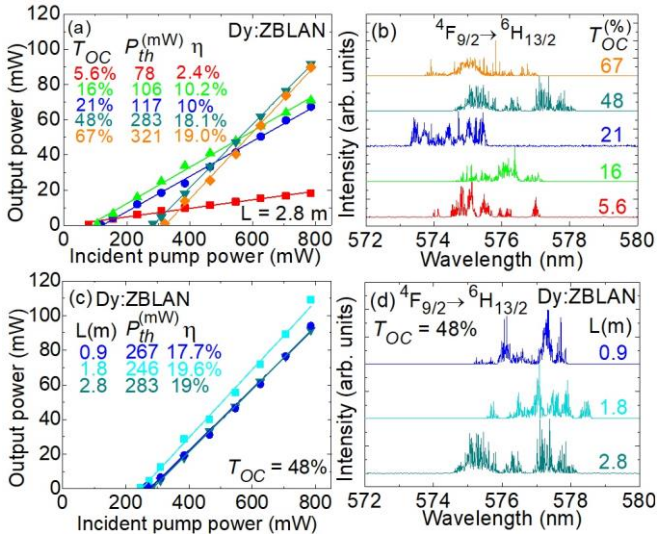

Fig. 3. Diode-pumped yellow Dy:ZBLAN fiber laser: (a,c) input-output dependences and (b,d) typical spectra of laser emission measured at P_{inc} = 785 mW for (a) different output coupling rates T_{OC}, and (c) various fiber lengths L, η – slope efficiency, P_{th} – laser threshold.

The Dy:ZBLAN fiber laser operated in the CW regime (only near the laser threshold, a strong tendency for self-pulsing behavior was noticed). First, the effect of the output coupling on the laser performance was studied for the longest available fiber (L = 2.8 m). The Dy-fiber laser generated a maximum output power of 92 mW at 575 nm with a slope efficiency η of 19% (versus incident pump power) and a laser threshold P_{th} of 283 mW for the high T_{OC} of 48%, Fig. 3(a). This corresponded to a maximum incident pump power P_{inc} of 785 mW and an optical efficiency of 11.7%. On increasing the output coupling, the laser threshold gradually increased from 78 mW (5.6% OC) to 321 mW (67% OC). The input-output dependences were linear and further power scaling was limited by the available pump. The typical spectra of laser emission measured at the maximum P_{inc} are shown in Fig. 3(b), revealing a weak dependence on the output coupling. The laser operated for hours without any degradation of the output power nor beam quality.

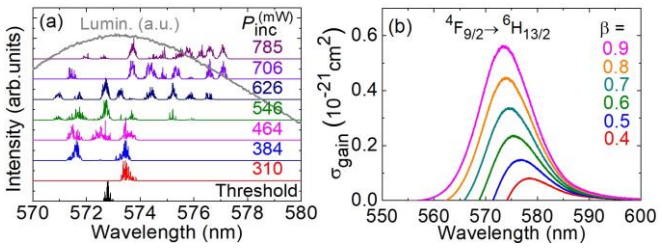

Fig. 4. Effect of the pump power on the spectral behavior of the Dy-fiber laser: (a) spectra of laser emission at various incident pump powers P_{inc}, *grey* curve - the luminescence spectrum shown for comparison; (b) gain cross-sections, $\sigma_{gain} = \beta\sigma_{SE} - (1-\beta)\sigma_{ESA}$, for the $^4F_{9/2} \leftrightarrow {}^6H_{13/2}$ transition of Dy^{3+} ions for different population inversions β. T_{OC} = 48%, L = 1.8 m.

Then, the fiber length was varied to find an optimum geometry in terms of competition of reduced losses as well as weaker pump absorption for shorter fibers. The output coupling was fixed at 48%. For the optimum fiber length L of 1.8 m, the Dy-fiber laser delivered 109 mW at 575 nm with a slightly improved η of 19.6% and a lower P_{th} of 246 mW (as compared to the longest fiber), see Fig. 3(c,d). This corresponded to an optical efficiency of 13.9%. The slope efficiency with respect to the absorbed pump power was 20.7%.

The evolution of the laser spectra with pump power is analyzed in Fig. 4(a). On increasing P_{inc}, the spectra broadened, and the center emission wavelength experienced a slight red shift from 572 nm to 575 nm. The former effect is explained by the gain saturation, and broad and smooth emission profiles of Dy^{3+} in ZBLAN. The multiple emission lines originate from the etalon effects at the fiber / mirror interfaces. To explain the shift of the laser wavelength, we calculated the gain cross-sections, $\sigma_{gain} = \beta\sigma_{SE} - (1-\beta)\sigma_{ESA}$, Fig. 4(b), accounting for the ESA from the terminal laser level, $^6H_{13/2} \rightarrow {}^4F_{9/2}$, Fig. 1(a), where N_1, N_2 and N_3 are the populations of the $^6H_{15/2}$, $^6H_{13/2}$ and $^4F_{9/2}$ manifolds, respectively, ($N_1 + N_2 + N_3 \approx N_{Dy}$) and $\beta = N_3/(N_2 + N_3)$ is the inversion ratio. For smaller inversion ratios, the maximum in the gain profiles shifts to longer wavelengths due to increased reabsorption caused by ESA. With increasing the pump power, the Dy^{3+} ions are accumulated in the long-living terminal laser level contributing to enhanced ESA at the laser wavelength.

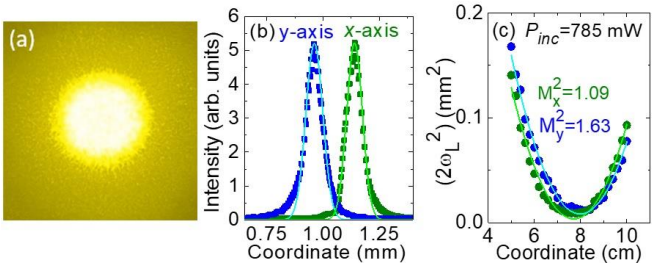

Fig. 5. Spatial characteristics of yellow emission from the Dy fiber laser: (a) a photograph of the yellow laser beam in the far-field; (b) 1D intensity profiles along the horizontal (x) and vertical (y) directions, *points* - experimental data, *lines* – their Gaussian fits; (c) evaluation of the beam quality factors $M^2_{x,y}$, P_{inc} = 785 mW, L = 1.8 m, T_{OC} = 48%.

A photograph of the yellow laser beam on a screen in the far-field is shown in Fig. 5(a), and the corresponding 1D intensity profiles together with their Gaussian fits are given in Fig. 5(b). The beam quality factors of laser emission at the maximum incident pump power of 785 mW were measured by an ISO-standard method, cf. Fig. 5(c), yielding M^2_x = 1.50 and M^2_y = 1.55. Despite the fiber core being multimode at 575 nm, the Dy-fiber laser exhibited a relatively good output beam quality. We attribute this to the high brightness of the used pump source resulting in predominant excitation of low-order modes in the fiber core. In comparison, Zou *et al.* used a low-brightness high-power 450-nm GaN diode module for pumping a similar Dy-fiber resulting in poorer beam quality of the laser emission ($M^2 \sim 6$) [14].

The round-trip passive losses in the fiber were estimated using the Findlay-Clay analysis, yielding L = 27.7%, or 0.22 dB/m at 575 nm. Note that this value includes the reabsorption loss at the laser wavelength caused by ESA.

The output performance of the Dy-fiber laser was simulated using the model of Kelson and Hardy [18]. The spectroscopic parameters determined in the present work, as well as the cavity characteristics described above were used. Both the pump and the laser radiation propagate in the core and the considered mode is LP_{01}. The rate-equation model takes into account ground-state

absorption at λ_P, stimulated emission and spontaneous emission into the laser mode, as well as excited-state absorption at λ_L. Solving the steady-state rate equations and propagation equations for the pump and laser was made through numerical methods, employing the fourth-order Runge-Kutta algorithm [19].

The effects of the variation of the output coupling and fiber length on the laser performance were studied when accounting for both ESA and propagation losses, Fig. 6(a,b). Our model agrees well with the experiment. It predicts an optimum output coupling about 32%, dictated mostly by the propagation losses in the fiber. There also exists an optimum fiber length L ~1.3 m, which is determined by a counterplay between the sufficiently high pump absorption and increasing overall losses in long fibers. The impact of ESA on the laser performance is significant and more than 2-fold improvement of the output power is expected if the population of the terminal laser level is drained thus preventing the ESA. Our model also allows for estimating the fractional populations of the upper and lower laser levels. For the 1.8 m-long fiber, at the maximum applied pump power, one finds N_2 = 0.18 and N_3 = 0.28 (β = 0.61) at the pumped end-facet of the fiber.

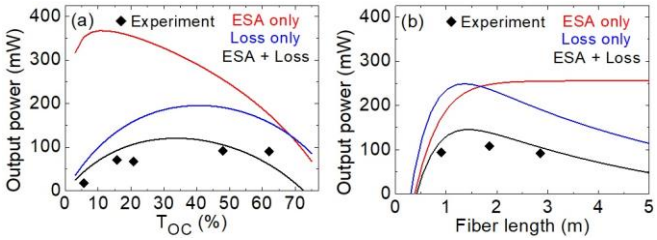

Fig. 6. Simulation of the output performance of a diode-pumped yellow Dy:ZBLAN fiber laser: (a) output power vs. output coupling rate T_{OC}, L = 2.8 m; (b) output power vs. fiber length L, T_{OC} = 48%. P_{inc} = 785 mW. *Red* and *blue* curves show the simulations considering only ESA and losses, respectively. Losses: 0.27 dB/cm (laser), 0.35 dB/cm (pump).

Previous research has documented the propensity for self-pulsing in Dy lasers [5]. This phenomenon has also been witnessed in other rare-earth ion lasers emitting in the visible [20] and was attributed to excited-state absorption at the laser wavelength acting as a "fast" artificial saturable absorber. ESA can occur from both the upper and lower laser levels. The latter case is observed only if the terminal multiplet has a non-negligible lifetime as in the case of Dy^{3+}. Notably, self-pulsing in Dy lasers based on high-phonon-energy oxide crystals [9] has not been reported, likely due to the strong non-radiative path from the lower laser level. For fluoride single crystals, it was shown that codoping with Tb^{3+} or Eu^{3+} ions could help to reduce the $^6H_{13/2}$ Dy^{3+} lifetime [5,10].

To conclude, we have successfully demonstrated a proof-of-concept of a simple and efficient yellow Dy:ZBLAN fiber laser with high-brightness pumping by two polarization-combined single-emitter 450-nm blue GaN diodes. This laser delivers >100 mW output at 575 nm with an overall optical efficiency of 13.9% being record-high for yellow Dy-fiber lasers, a low laser threshold and a high beam quality. The output performance of the Dy-fiber laser is simulated accounting for the propagation losses in the fiber (estimated as 0.22 dB/m at 575 nm, reabsorption losses included) and resonant ESA from the terminal laser level. We show that both these factors determine the optimum laser design in terms of the fiber length and output coupling. ESA appears to be a major limiting factor for enhancing the laser slope efficiency. Two strategies are envisioned to overcome this issue: i) cascade lasing in the yellow and mid-infrared spectral ranges (on the $^4F_{9/2} \rightarrow {}^6H_{13/2}$ and $^6H_{13/2} \rightarrow {}^6H_{15/2}$ sequent transitions) and ii) codoping of the fiber core with a small amount of Tb^{3+} or Eu^{3+} ions for quenching of the $^6H_{13/2}$ level lifetime. The latter approach would require a detailed spectroscopic study of codoped ZBLAN glasses.

Funding. Normandy region (FIZIC project; Contrat de plan État-Région (CPER)); Agence Nationale de la Recherche (ANR-22-CE08-0025-01, NOVELA).

Acknowledgements. This Project was supported in a joint framework between the French State, under the Future Investments Program, and the Normandy region (FIZIC project).

Disclosures. The authors declare no conflicts of interest.

Data availability. Data underlying the results presented in this paper are not publicly available at this time but may be obtained from the authors upon reasonable request.

References

1. N. K. Yadav, C. Jayadev, A. Mohan, P. Vijayan, R. Battu, S. Dabir, B. Shetty, and R. Shetty, Eye **29**, 258-265 (2015).
2. X. Yang, O. Kitzler, D. J. Spence, Z. Bai, Y. Feng, and R. P. Mildren, Opt. Lett. **45**, 1898-1901 (2020).
3. H.M. Pask and J. A. Piper, Optics letters, Opt. Lett. **24**(21), 1490-1492 (1999).
4. H. Zhu, Y. Duan, G. Zhang, C. Huang, Y. Wei, W. Chen, Y. Huang, and N. Ye, Opt. Lett. **34**, 2763-2765 (2009).
5. C. Kränkel, D. T. Marzahl, F. Moglia, G. Huber and P. W. Metz, Laser & photonics reviews **10**(4), 548-568 (2016).
6. M. Z. Amin, S. D. Jackson, and M. R. Majewski, Appl. Opt. **60**(16), 4613-4621 (2021).
7. R. Piramidowicz, M. Klimczak and M. Malinowski, Opt. Mat. **30**(5), 707-710 (2008).
8. J. S. Kumar, K. Pavani, A. M. Babu, N. K. Giri, S. B. Rai and L. R. Moorthy, Journal of Luminescence **130**(10), 1916-1923 (2010).
9. S. R. Bowman, S. O'Connor, and N. J. Condon, Opt. Express **20**, 12906-12911 (2012).
10. G. Bolognesi, D. Parisi, D. Calonico, G. A. Costanzo, F. Levi, P. W. Metz, C. Kränkel, G. Huber and M. Tonelli, Opt. Lett. **39**(23), 6628-6631 (2014).
11. J. Limpert, H. Zellmer, P. Riedel, G. Maze, and A. Tunnermann, Electron. Lett. **36**, 1386–1387 (2000).
12. T. Okazaki, C. Otsuka, E. H. Sekiya, K. Kawai, M. Mizusaki, Y. Kanbayashi and K. Saito, App. Phys. Express **15**(1), 012002 (2021).
13. H. Wang, J. Zou, C. Dong, T. Du, B. Xu, H. Xu, Z. Cai, and Z. Luo, Opt. Lett. **44**(17), 4423-4426 (2019).
14. J. Zou, T. Li, Y. Dou, J. Li, N. Chen, Y. Bu, and Z. Luo, Photon. Res. **9**(4), 446-451 (2021).
15. K. Takahashi, N. Nashimoto, A. Koganei, H. Katsuragawa, Y. Fujimoto, O. Ishii and M. Yamazaki, Opt. Comm. **545**, 129650 (2023).
16. S. Aasland, M. A. Einarsrud, T. Grande and P. F. McMillan, J. Phys. Chem. **100**(13), 5457-5463 (1996).
17. L. Gomes, A. F. H. Librantz, S. D. Jackson, J. Appl. Phys. **107**(5), 053103 (2010).
18. I. Kelson and A. A.Hardy, IEEE Journal of Quantum Electronics **34**(9), 1570-1577 (1998).
19. E. Kifle, F. Starecki, P. Loiko, S. Cozic, F. Joulain, T. Berthelot, T. Georges, D. Stojcevski, D. Deubel, and P. Camy, Opt. Lett. **46**(1), 74-77 (2021).
20. A. Baillard, P. Loiko, D. Rytz, S. Schwung, M. Fromager, A. Braud, and P. Camy, Opt. Lett. **48**(18), 4721-4724 (2023).

Full references

1. N. K. Yadav, C. Jayadev, A. Mohan, P. Vijayan, R. Battu, S. Dabir, B. Shetty, and R. Shetty. "Subthreshold micropulse yellow laser (577 nm) in chronic central serous chorioretinopathy: safety profile and treatment outcome." Eye **29**, 258-265 (2015).
2. X. Yang, O. Kitzler, D. J. Spence, Z. Bai, Y. Feng, and R. P. Mildren, "Diamond sodium guide star laser," Opt. Lett. **45**, 1898-1901 (2020).
3. H.M. Pask and J. A. Piper, Optics letters, "Efficient all-solid-state yellow laser source producing 1.2-W average power," Opt. Lett. **24**(21), 1490-1492 (1999).
4. H. Zhu, Y. Duan, G. Zhang, C. Huang, Y. Wei, W. Chen, Y. Huang, and N. Ye, "Yellow-light generation of 5.7 W by intracavity doubling self-Raman laser of YVO_4/Nd:YVO_4 composite," Opt. Lett. **34**, 2763-2765 (2009).
5. C. Kränkel, D. T. Marzahl, F. Moglia, G. Huber and P. W. Metz, "Out of the blue: semiconductor laser pumped visible rare-earth doped lasers," Laser & photonics reviews **10**(4), 548-568 (2016).
6. M. Z. Amin, S. D. Jackson, and M. R. Majewski, "Experimental and theoretical analysis of Dy^{3+}-doped fiber lasers for efficient yellow emission," Appl. Opt. **60**(16), 4613-4621 (2021).
7. R. Piramidowicz, M. Klimczak and M. Malinowski, "Short-wavelength emission analysis in Dy:ZBLAN glasses" Opt. Mat. **30**(5), 707-710 (2008).
8. J. S. Kumar, K. Pavani, A. M. Babu, N. K. Giri, S. B. Rai and L. R. Moorthy, "Fluorescence characteristics of Dy^{3+} ions in calcium fluoroborate glasses," Journal of Luminescence **130**(10), 1916-1923 (2010).
9. S. R. Bowman, S. O'Connor, and N. J. Condon, "Diode pumped yellow dysprosium lasers," Opt. Express **20**, 12906-12911 (2012).
10. G. Bolognesi, D. Parisi, D. Calonico, G. A. Costanzo, F. Levi, P. W. Metz, C. Kränkel, G. Huber and M. Tonelli, "Yellow laser performance of Dy^{3+} in co-doped Dy,Tb:$LiLuF_4$," Opt. Lett. **39**(23), 6628-6631 (2014).
11. J. Limpert, H. Zellmer, P. Riedel, G. Maze, and A. Tunnermann, "Laser oscillation in yellow and blue spectral range in Dy^{3+}:ZBLAN," Electron. Lett. **36**, 1386–1387 (2000).
12. T. Okazaki, C. Otsuka, E. H. Sekiya, K. Kawai, M. Mizusaki, Y. Kanbayashi and K. Saito, "Diode pumped visible Dy^{3+}-doped silica fiber laser: Ge-co-doping effects on lasing efficiency and photodarkening," App. Phys. Expr., **15**(1), 012002 (2021).
13. H. Wang, J. Zou, C. Dong, T. Du, B. Xu, H. Xu, Z. Cai, and Z. Luo, "High-efficiency, yellow-light Dy^{3+}-doped fiber laser with wavelength tuning from 568.7 to 581.9 nm," Opt. Lett. **44**(17), 4423-4426 (2019).
14. J. Zou, T. Li, Y. Dou, J. Li, N. Chen, Y. Bu, and Z. Luo, "Direct generation of watt-level yellow Dy^{3+}-doped fiber laser," Photon. Res. **9**(4), 446-451 (2021).
15. K. Takahashi, N. Nashimoto, A. Koganei, H. Katsuragawa, Y. Fujimoto, O. Ishii and M. Yamazaki, "Development of a primary yellow (575 nm) laser by Dy^{3+}-doped double-clad-structured waterproof fluoro-aluminate glass fiber" Opt. Comm. **545**, 129650 (2023).
16. S. Aasland, M. A. Einarsrud, T. Grande and P. F. McMillan, "Spectroscopic investigations of fluorozirconate glasses in the ternary systems ZrF_4-BaF_2-AF (A= Na, Li)," J. Phys. Chem., **100**(13), 5457-5463 (1996).
17. L. Gomes, A. F. H. Librantz, S. D. Jackson, "Energy level decay and excited state absorption processes in dysprosium-doped fluoride glass," J. Appl. Phys. **107**(5), 053103 (2010).
18. I. Kelson and A. A.Hardy, "Strongly pumped fiber lasers," IEEE Journal of Quantum Electronics, **34**(9), 1570-1577 (1998).
19. E. Kifle, F. Starecki, P. Loiko, S. Cozic, F. Joulain, T. Berthelot, T. Georges, D. Stojcevski, D. Deubel, and P. Camy, "Watt-level visible laser in double-clad Pr^{3+}-doped fluoride fiber pumped by a GaN diode," Opt. Lett. **46**(1), 74-77 (2021).
20. A. Baillard, P. Loiko, D. Rytz, S. Schwung, M.Fromager, A. Braud, and P. Camy, "Red Sm:$KGd(WO_4)_2$ laser at 649 nm," Opt. Lett. **48**(18), 4721-4724 (2023).